18th Brazilian Congress of Thermal Sciences and Engineering
November 16-20, 2020 (Online)

# ENC-2020-0194
# NUMERICAL SIMULATION OF AÇAÍ SEED AND MUNICIPAL SOLID WASTE DOWNDRAFT CO-GASIFICATION

**Caroline Smith Lewin**
**Florian Pradelle**
Departamento de Engenharia Mecânica (DEM), Pontifícia Universidade Católica do Rio de Janeiro (PUC-Rio), Rio de Janeiro, RJ Brazil
carolineslewin@gmail.com; pradelle@puc-rio.br

**Ana Rosa Fonseca de Aguiar Martins**
Departamento de Engenharia Química e de Materiais (DEQM), Pontifícia Universidade Católica do Rio de Janeiro (PUC-Rio), Rio de Janeiro, RJ Brazil
anarosa@puc-rio.br

***Abstract.*** *The purpose of this study was to simulate the downdraft co-gasification of açaí seed and municipal solid waste. The choice of biomasses highlights the "Waste to Energy concept", investigating the potential for energy generation of an important Brazilian agro-industrial residue and the waste produced by urban activities. A previously developed kinetic model was employed, taking into account the effects of moisture evaporation, pyrolysis, combustion and gasification chemical reactions. A central composite design of experiments using the co-gasification ratio and the equivalence ratio as factors was performed, and some statistical analyses were carried out. Polynomial models were developed for the sum of CO and $H_2$ molar fractions, the lower heating value of the syngas and the energy efficiency. The optimized condition corresponded to the gasification of açaí seed alone with an equivalence ratio of 0.18, and produced a syngas with a sum of CO and $H_2$ of 45.5%, a lower heating value of 5.98 MJ/kg and an energy efficiency of 32.2%. These results were used for comparison to other conditions, such as the gasification of sugarcane bagasse, and the co-gasification of 40% municipal solid waste with both açaí seed and bagasse and 0.15 equivalence ratio.*

***Keywords:*** *gasification, açaí seed, municipal solid waste, kinetic modelling*

## 1. INTRODUCTION

This work aimed to apply a previous model of a gasifier operating with air and in downdraft configuration using a kinetic, one-dimensional and steady state approach (Lewin et al., 2020). The model was used to simulate the co-gasification of açaí seed and municipal solid waste (MSW), and the potential for energy generation of different percentages of this combination of biomasses was investigated. The comparison of MSW co-gasification with açaí seed and sugarcane bagasse, the latter studied in a previous work (Lewin et al., 2020), was also addressed. In addition to a cleaner energy production in comparison to fossil fuels, the gasification of residues also proposes an alternative to the environmental problems concerning waste disposal, as well as the lack of available field.

Açaí berry (*Euterpe oleracea Mart.*) is native of Amazon and is widely produced in the North of Brazil. According to the National Supply Company (CONAB, 2019), the state of Pará is the world's major producer and Brazilian exporter of açaí, followed by the state of Amazonas. According to the Brazilian Institute of Geography and Statistics (IBGE), Brazil produced over 1.5 million tonnes of açaí in the year of 2018 and the state of Pará alone was responsible for 95.3% of this production. The national production of this fruit increased in almost 50% compared to the year of 2015, and in over 13% when compared to 2017 (IBGE/PAM, 2019). However, the pulp, which is the consumed part of açaí, consists only of 6.7 to 19.7% on a weight basis of the fruit, the rest being seed and peel (Monteiro et al., 2017).

MSW disposal is an environmental concern worldwide and its generation comes from household and commercial activities (Speight, 2010). Along with the worldwide growth of urban population over the years, the production per capita of MSW also increases (Hoornweg and Bhada-Tata, 2012). In Brazil, almost 60% of MSW that is collected is sent to landfills, whereas a remarkable amount of this waste is not even collected and has inappropriate destinations (ABRELPE, 2017). The landfills themselves are not considered as environmentally adequate since they are potential generators of pollutants like methane. Both açaí seed and MSW are, therefore, important residues for the "Waste to Energy" concept in Brazil.

In downdraft (cocurrent) gasification, both biomass and gasifying agent are fed at the top of the reactor. Even though this process has lower thermal efficiency than updraft (countercurrent) gasification, it has the advantage to produce a

cleaner synthesis gas (syngas) with low tar content. It happens because the biomass devolatilization products reach high temperatures passing through combustion zone and tar can be converted, whereas this does not happen in updraft gasifiers. This makes downdraft gasifiers more suitable for advanced applications (Ptasinski, 2016, Lasa et al., 2011 and Situmorang et al., 2020).

Most of the studies on downdraft gasification modelling by a kinetic approach considers a steady state operation. Rodrigues *et al.* (2009) investigated a one-dimensional gasifier-combustion unit of solid wastes from footwear industries. Giltrap *et al.* (2003) modeled a one-dimensional reduction zone of a downdraft gasifier considering four chemical reactions. There was an over-prediction of $CH_4$ in syngas, which led them to propose, in a previous work based in the same model, an additional combustion reaction of $CH_4$ (Giltrap, 2002). Chaurasia (2014) also formulated a one-dimensional model for downdraft gasification, in which combustion and reduction gasifier zones were considered, along with tar pyrolysis. The pyrolysis of biomass, however, was not modeled and its products were calculated from a given variable called pyrolysis fraction, varying from 0 to 1. Other studies formulated models for unsteady state downdraft gasifiers. DiBlasi (2000) investigated the dynamic one-dimensional gasification of woody biomass in a stratified reactor. Lastly, Yucel and Hastaoglu (2016) modeled a transient throated gasifier of wood pellets and conducted an experimental validation, also in one dimension.

## 2. METHODOLOGY

### 2.1 Gasifier modeling

The downdraft gasifier was modelled using species, mass and energy conservation equations written in differential form, for both solid and gas phase. A steady-state, unidimensional approach was conducted and equations for transport phenomena were used, including Arrhenius type kinetic equations and heat transport equations between the phases and the gasifier wall. The problem was solved with respect to the position in the gasifier using the ode23 function available in MATLAB®, which solves differential equations by implementing explicit Runge-Kutta (2,3) (Lewin et al., 2020). Table 1 presents elemental composition, moisture content, higher heating value and bulk density of both types of biomass and Tab. 2 shows the chemical reactions considered in the model.

Table 1. Biomass characterization (elemental composition on a weight, dry basis)

| | C (%) | H (%) | O (%) | N (%) | S (%) | Ash (%) | Moisture content (%) | Higher heating value (kJ/kg) | Bulk density (kg/m$^3$) |
|---|---|---|---|---|---|---|---|---|---|
| **Açaí seed (Santos, 2011)** | 46.04 | 6.77 | 38.3 | 7.99 | 0.08 | 1.39 | 15.5 | 18,141 | 473.92 |
| **MSW (Leme et al., 2014 ; Angelo et al., 2017)** | 40.00 | 5.00 | 25.00 | 1.00 | 0.20 | 28.00 | 37.0 | 13,064 | 1000 |

Table 2. Chemical reactions

| | | |
|---|---|---|
| **Evaporation (m)** | $H_2O_{(l)} \rightarrow H_2O_{(g)}$ | (1) |
| **Biomass pyrolysis (p1)** | $B \rightarrow 0.350char + 0.045CO + 0.100CO_2 + 0.002H_2 + 0.003CH_4 + 0.115H_2O + 0.385tar$ (2) | (2) |
| **Tar pyrolysis (p2)** | $tar \rightarrow 0.534CO + 0.085CO_2 + 0.211CH_4$ (3) | (3) |
| **Water-gas shift reaction (wg)** | $CO + H_2O \leftrightarrow CO_2 + H_2$ | (4) |
| **Boudouard reaction (g1)** | $C + CO_2 \rightarrow 2CO$ | (5) |
| **$H_2O$ gasification (g2)** | $C + H_2O \rightarrow CO + H_2$ | (6) |
| **Methanation reaction (g3)** | $C + 2H_2 \rightarrow CH_4$ | (7) |
| **$CH_4$ and $H_2O$ reaction (g4)** | $CH_4 + H_2O \rightarrow CO + 3H_2$ | (8) |
| **$CH_4$ combustion (c1)** | $CH_4 + 2O_2 \rightarrow CO_2 + 2H_2O$ | (9) |
| **CO combustion (c2)** | $2CO + O_2 \rightarrow 2CO_2$ | (10) |
| **$H_2$ combustion (c3)** | $2H_2 + O_2 \rightarrow 2H_2O$ | (11) |

Table 3 presents the rates and specific rates of the chemical reactions, as well as their equilibrium constants and reaction heats $\Delta H_{j,ref}$ . $P_i$ is species i partial pressure in bar, R is the universal constant of perfect gases in J mol$^{-1}$ K$^{-1}$ and T is the temperature in K of either solid or gas phase.

Table 3. Kinetic parameters (Lewin et al., 2020)

| **Reaction rate $R_j$** | **Specific rate $k_j$ and equilibrium constant $K_j$** | $\Delta H_{j,ref}$ | **Ref.** |
|---|---|---|---|
| $R_m = k_m \rho_M$ (12) | $k_m = 5.13 \times 10^{10}\, exp\left(\frac{-88 \times 10^3}{RT_s}\right)$ (13) | 2250 kJ/kg | Bryden et al., 2002; Mandl et al., 2010 |
| $R_{p1} = k_{p1} \rho_B$ (14) | $k_{p1} = 7.41 \times 10^4 exp\left(\frac{-83.6 \times 10^3}{RT_s}\right)$ (15) | -420 kJ/kg | Mandl et al., 2010; DiBlasi, 2000 |
| $R_{p2} = k_{p2} \rho_{tar}$ (16) | $k_{p2} = 4.28 \times 10^6 exp\left(\frac{-107 \times 10^3}{RT_g}\right)$ (17) | 42 kJ/kg | DiBlasi, 2000 |
| $R_{wg} = k_{wg}\left(C_{CO}C_{H2O} - \frac{C_{CO2}C_{H2}}{K_E}\right)$ (18) | $k_{wg} = 2.78\, exp\left(\frac{-12.6 \times 10^3}{RT_g}\right)$ (19)<br>$K_E = 0.02565\, exp\left(\frac{32.97 \times 10^3}{RT_g}\right)$ (20) | -41.98 kJ/mol | DiBlasi, 2004; Basu, 2006 apud Rodrigues, 2008 |
| $R_{g1} = k_{g1}\left(P_{CO2} - \frac{P_{CO}^2}{K_{g1}}\right)$ (21) | $k_{g1} = 36.16\, exp\left(\frac{-77.39 \times 10^3}{RT_s}\right)$ (22)<br>$log_{10}K_{g1} = -\frac{8900}{T_s} + 9.1$ (23) | 172.6 kJ/mol | Giltrap, 2002; DiBlasi, 2004 |
| $R_{g2} = k_{g2}\left(P_{H2O} - \frac{P_{CO}P_{H2}}{K_{g2}}\right)$ (24) | $k_{g2} = 1.517 \times 10^4 exp\left(\frac{-121.62 \times 10^3}{RT_s}\right)$ (25)<br>$log_{10}K_{g2} = -\frac{7000}{T_s} + 7.4$ (26) | 131.4 kJ/mol | Giltrap, 2002; DiBlasi, 2004 |
| $R_{g3} = k_{g3}\left(P_{H2}^2 - \frac{P_{CH4}}{K_{g3}}\right)$ (27) | $k_{g3} = 4.189 \times 10^{-3} exp\left(\frac{-19.21 \times 10^3}{RT_s}\right)$ (28)<br>$log_{10}K_{g3} = \frac{4400}{T_s} - 5.5$ (29) | -74.93 kJ/mol | Giltrap, 2002; DiBlasi, 2004 |
| $R_{g4} = k_{g4}\left(P_{CH4}P_{H2O} - \frac{P_{CO}P_{H2}^3}{K_{g4}}\right)$ (30) | $k_{g4} = 7.301 \times 10^{-2} exp\left(\frac{-36.15 \times 10^3}{RT_g}\right)$ (31)<br>$log_{10}K_{g4} = -\frac{11370}{T_g} + 12.878$ (32) | 206 kJ/mol | Giltrap, 2002 |
| $R_{c1} = k_{c1}\left(P_{CH4}P_{O2}^2 - \frac{P_{CO2}P_{H2O}^2}{K_{c1}}\right)$ (33) | $k_{c1} = 29.71\, exp\left(\frac{-22.028 \times 10^3}{RT_g}\right)$ (34)<br>$log_{10}K_{c1} = \frac{41837}{T_g} - 0.0273$ (35) | -805 kJ/mol | Giltrap, 2002; DiBlasi, 2000 |
| $R_{c2} = k_{c2}\left(P_{O2}P_{CO}^2 - \frac{P_{CO2}^2}{K_{c2}}\right)$ (36) | $k_{c2} = 1.215 \times 10^6 exp\left(\frac{-125.58 \times 10^3}{RT_g}\right)$ (37)<br>$log_{10}K_{c2} = \frac{29573}{T_g} - 9.1017$ (38) | -283.03 kJ/mol | Estimated; DiBlasi, 2004; Higman, 2003 apud Rodrigues, 2008 |
| $R_{c3} = k_{c3}\left(P_{O2}P_{H2}^2 - \frac{P_{H2O}^2}{K_{c3}}\right)$ (39) | $k_{c3} = 1.565 \times 10^4 exp\left(\frac{-83.14 \times 10^3}{RT_g}\right)$ (40)<br>$log_{10}K_{c3} = \frac{25587}{T_g} - 5.5441$ (41) | -241.8 kJ/mol | Estimated; Chaurasia, 2016; Higman, 2003 apud Rodrigues, 2008 |

The differential equations of species conservation in both phases are summarized below. The constituent species solid phase are biomass, moisture and char, and the constituents of gas phase are tar, $H_2O$, $O_2$, CO, $CO_2$, $H_2$, $CH_4$ and $N_2$. The index j represents reactions wg, g1, g2, g3, g4, c1, c2 and c3. The mass concentration of each is species i is represented by $\rho_i$ and the velocity of solid and gas phases are represented by $U_s$ and $U_g$, respectively. $\nu_{i,j}$ is the stoichiometric coefficient of species i in reaction j.

$$\frac{\partial(\rho_i U_s)}{\partial z} = M_i \sum_j \nu_{i,j} R_j + \nu_{i,p1} R_{p1} + \nu_{i,p2} R_{p2} + \nu_{i,m} R_m \quad (42)$$

$$\frac{\partial(\rho_i U_g)}{\partial z} = M_i \sum_j \nu_{i,j} R_j + \nu_{i,p1} R_{p1} + \nu_{i,p2} R_{p2} + \nu_{i,m} R_m \quad (43)$$

Solid velocity was modelled as constant until the start of char gasification reactions, and gas velocity was evaluated through a balance between the phases (Ismail and El-Salam, 2017). The Ergun equation was employed to evaluate pressure drop in the gasifier (Chaurasia, 2016).

$$\frac{\partial U_s}{\partial z} = \frac{1}{\rho_{char0}} M_{char}\left(\nu_{char,g1} R_{g1} + \nu_{char,g2} R_{g2} + \nu_{char,g3} R_{g3}\right) \quad (44)$$

$$\varepsilon \frac{\partial \rho_g U_g}{\partial z} + (1-\varepsilon)\frac{\partial \rho_s U_s}{\partial z} = 0 \quad (45)$$

Lastly, the energy equations are presented. The axial conductive term could be neglected since the value of Peclet number was above 100 after the first 10 cm of the gasifier, meaning that the axial conduction is negligible (Bejan, 2013). The reactions j considered in solid energy equation are m, p1, g1, g2 and g3, and in the gas energy equation are wg, p2, g4, c1, c2 and c3.

$$\frac{\partial(U_s \sum_i \rho_i H_{si})}{\partial z} = \frac{\partial}{\partial z}\left(\lambda_s \frac{\partial T_s}{\partial z}\right) - \sum_j R_j \Delta H_j - Q_{sg} - Q_{sw} \quad (46)$$

$$\frac{\partial(U_g \sum_i \rho_i H_{gi})}{\partial z} = \frac{\partial}{\partial z}\left(\lambda_g \frac{\partial T_g}{\partial z}\right) - \sum_j R_j \Delta H_j + Q_{sg} - Q_{gw} \quad (47)$$

### 2.2 Central composite design of experiments

A central composite design of experiments was used to extract as many information as possible of the simulations. The effects of two factors on the gasification process were studied, each one of them in three levels ($3^2$). The first variable under study was the co-gasification ratio (CGR), which measures the ratio of mass of municipal solid waste to the total mass of the mixture, composed of açaí seed and municipal solid waste. The second variable under study was the equivalence ratio (ER), which is the real air to fuel ratio divided by the stoichiometric air to fuel ratio. Table 4 summarizes the factors and their levels.

Table 4. Factors of the design of experiments and their levels

| Factor | Name | Level -1 | Level 0 | Level +1 |
|---|---|---|---|---|
| $x_1$ | **CGR** | 0% | 20% | 40% |
| $x_2$ | **ER** | 0.18 | 0.20 | 0.22 |

After the 9 corresponding simulations, polynomial models and statistical analyses such as analysis of variance (ANOVA) and analysis of coefficients were conducted so that conclusions regarding the efficiency of the gasification process could be made. Three main responses were chosen to characterize the process, the sum of CO and $H_2$ molar fractions on a wet basis, the lower heating value of the syngas on a dry basis and the energy efficiency on a dry basis, which is the ratio of the syngas LHV to the biomass LHV. The model equation for the quadratic polynomials is shown below.

$$y = a_0 + a_1 x_1 + a_{11} {x_1}^2 + a_2 x_2 + a_{22} {x_2}^2 + a_{12} x_1 x_2 \quad (48)$$

## 3. RESULTS

### 3.1 Simulations of the design of experiments

The downdraft co-gasification of municipal solid waste and açaí seed was simulated in a 50 cm length and 30 cm diameter reactor. A solid phase mass flow rate of 3 kg/h was used for simulations, and the gas flow rate was calculated according to the equivalence ratio. The results of the 9 simulations of the design of experiments is presented in Table 5.

Table 5. Results of the simulations of the design of experiments

| CGR (%) | ER | $H_2O$ | CO | $CO_2$ | $H_2$ | $CH_4$ | $N_2$ | CO+$H_2$ (%wb) | LHV (MJ/kg) db | Efficiency (%) db |
|---|---|---|---|---|---|---|---|---|---|---|
| **0** | **0.18** | 0.055 | 0.253 | 0.102 | 0.202 | 0.011 | 0.376 | 45.5 | 5.98 | 32.2 |
| **0** | **0.2** | 0.057 | 0.238 | 0.108 | 0.188 | 0.011 | 0.399 | 42.6 | 5.52 | 29.7 |
| **0** | **0.22** | 0.064 | 0.218 | 0.115 | 0.171 | 0.011 | 0.422 | 38.9 | 4.99 | 26.9 |
| **20** | **0.18** | 0.071 | 0.223 | 0.118 | 0.204 | 0.013 | 0.371 | 42.7 | 5.74 | 31.9 |
| **20** | **0.2** | 0.079 | 0.204 | 0.124 | 0.185 | 0.012 | 0.396 | 38.9 | 5.18 | 28.8 |
| **20** | **0.22** | 0.088 | 0.189 | 0.127 | 0.166 | 0.012 | 0.419 | 35.5 | 4.69 | 26.1 |
| **40** | **0.18** | 0.096 | 0.188 | 0.134 | 0.2 | 0.015 | 0.368 | 38.7 | 5.38 | 30.9 |
| **40** | **0.2** | 0.105 | 0.174 | 0.135 | 0.179 | 0.014 | 0.393 | 35.3 | 4.86 | 27.9 |
| **40** | **0.22** | 0.114 | 0.162 | 0.136 | 0.16 | 0.013 | 0.415 | 32.2 | 4.39 | 25.2 |

### 3.2 Statistical analyses

The analysis of variance is presented in Table 6. The significant coefficients based on a p-value below 5% are shown in bold. The complete models were also analysed, and in all cases the associated p-value was below 0.4%, showing the robustness of the polynomial models to predict the responses.

Table 6. ANOVA

| | | SS | DF | MS | F-ratio | p-value |
|---|---|---|---|---|---|---|
| **$CO+H_2$** | **$a_1$** | **71.9681** | **1** | **71.9681** | **852.8145** | **0.0001** |
| | $a_{11}$ | 0.0578 | 1 | 0.0578 | 0.6849 | 0.4686 |
| | **$a_2$** | **69.7004** | **1** | **69.7004** | **825.9431** | **0.0001** |
| | $a_{22}$ | 0.0012 | 1 | 0.0012 | 0.0148 | 0.9108 |
| | $a_{12}$ | 0.0025 | 1 | 0.0025 | 0.0296 | 0.8743 |
| | **Model** | 141.7300 | 5 | 28.3460 | 335.8974 | 0.0003 |
| | **Error** | 0.2532 | 3 | 0.0844 | | |
| | **Total** | 141.9832 | 8 | | | |
| **LHV** | **$a_1$** | **0.5770** | **1** | **0.5770** | **543.7426** | **0.0002** |
| | $a_{11}$ | 0.0007 | 1 | 0.0007 | 0.6815 | 0.4696 |
| | **$a_2$** | **1.5415** | **1** | **1.5415** | **1452.5374** | **0.0000** |
| | $a_{22}$ | 0.0002 | 1 | 0.0002 | 0.2192 | 0.6716 |
| | $a_{12}$ | 0.0000 | 1 | 0.0000 | 0.0011 | 0.9754 |
| | **Model** | 2.1195 | 5 | 0.4239 | 399.4363 | 0.0002 |
| | **Error** | 0.0032 | 3 | 0.0011 | | |
| | **Total** | 2.1227 | 8 | | | |
| **Energy efficiency** | **$a_1$** | **3.7871** | **1** | **3.7871** | **118.4956** | **0.0017** |
| | $a_{11}$ | 0.0345 | 1 | 0.0345 | 1.0794 | 0.3752 |
| | **$a_2$** | **47.6887** | **1** | **47.6887** | **1492.1614** | **0.0000** |
| | $a_{22}$ | 0.0081 | 1 | 0.0081 | 0.2536 | 0.6492 |
| | $a_{12}$ | 0.0340 | 1 | 0.0340 | 1.0648 | 0.3780 |
| | **Model** | 51.5524 | 5 | 10.3105 | 322.6110 | 0.0003 |
| | **Error** | 0.0959 | 3 | 0.0320 | | |
| | **Total** | 51.6483 | 8 | | | |

The coefficients for the polynomial models are presented in Table 7, along with their statistical analysis. Again, a p-value below 5% was considered for the significant coefficients, which are shown in bold in Table 7.

Table 7. Coefficients of the polynomial models of syngas sum of CO and $H_2$ molar fractions, syngas lower heating value and energy efficiency

| | **$CO+H_2$** | | | **LHV** | | | **Energy efficiency** | | |
|---|---|---|---|---|---|---|---|---|---|
| | **Coefficient** | **t-ratio** | **p-value** | **Coefficient** | **t-ratio** | **p-value** | **Coefficient** | **t-ratio** | **p-value** |
| **$a_0$** | **39.0500** | **180.35** | **0.00000** | **5.1967** | **214.02** | **0.00000** | **28.8812** | **216.75** | **0.00000** |
| **$a_1$** | **-3.4633** | **-29.20** | **0.00009** | **-0.3101** | **-23.32** | **0.00017** | **-0.7945** | **-10.89** | **0.00166** |
| **$a_{11}$** | -0.1700 | -0.83 | 0.46858 | -0.0190 | -0.83 | 0.46959 | -0.1313 | -1.04 | 0.37520 |
| **$a_2$** | **-3.4083** | **-28.74** | **0.00009** | **-0.5069** | **-38.11** | **0.00004** | **-2.8192** | **-38.63** | **0.00004** |
| **$a_{22}$** | -0.0250 | -0.12 | 0.91083 | 0.0108 | 0.47 | 0.67158 | 0.0637 | 0.50 | 0.64921 |
| **$a_{12}$** | 0.0250 | 0.17 | 0.87430 | -0.0005 | -0.03 | 0.97544 | -0.0922 | -1.03 | 0.37803 |

The significant coefficients are the independent ($a_0$) and the linear coefficients of both effects ($a_1$ and $a_2$) in all the chosen responses, which suggests that the model could have been developed for a linear polynomial. Since their values

are negative and this analysis is done using the dimensionless values of variables, it can be concluded that all of them have an inhibiting effect on the responses. This means that increasing the CGR results in a decrease of the syngas sum of CO and $H_2$ molar fractions, of the syngas lower heating value and or the energy efficiency. An increase in CGR corresponds to an increase of the amount of MSW, so it is expected that the lowest amount of MSW provides the best results. The same can be concluded for the ER, and the lowest amount of air is preferable for the co-gasification of these two biomasses.

The polynomial models enabled the calculation of the predicted results of the sum of CO and $H_2$ molar fractions, the heating value and the energy efficiency. These are presented in Figure 1. The good agreement between the observed and calculated results and the high values of $R^2$ and adjusted $R^2$ show that that the polynomial models of all responses are robust.

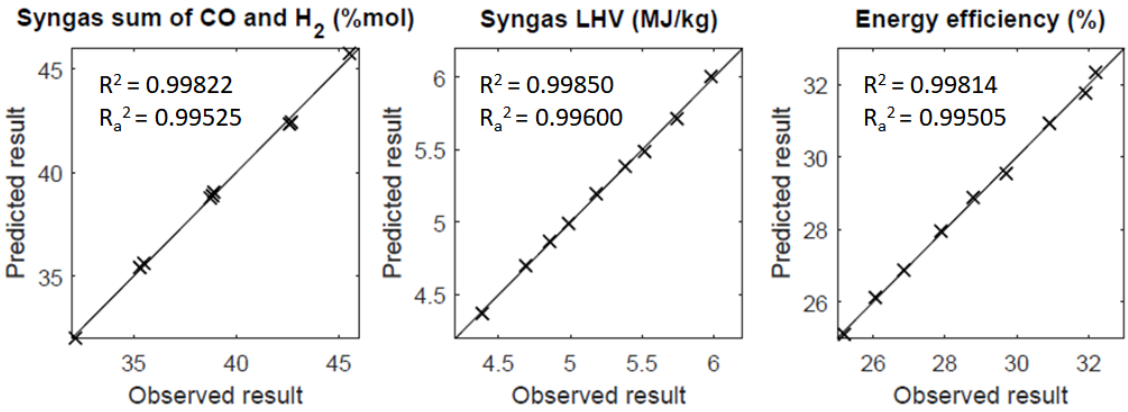


Figure 1. Predicted by polynomial models versus observed by MATLAB model results and their corresponding $R^2$ and $R_a^2$

### 3.3 Optimization of co-gasification conditions

The response surfaces of the three polynomial models are shown in Figure 2. As expected and already commented, the results are maximized for CGR 0% and ER 0.18. The high moisture content of municipal solid waste (37.0% as shown in Table 1) makes this residue a worse biomass for gasification in comparison to açaí seed (moisture content 15.5%). In addition, açaí seed is richer in elemental carbon and hydrogen, suggesting it can produce a higher quality syngas, maximizing the responses. The equivalence ratio of 0.18 means that the least amount of air results in more CO and $H_2$ and less combustion products, as $CO_2$ and $H_2O$, since less oxygen is available for reactions in this zone of the gasifier.

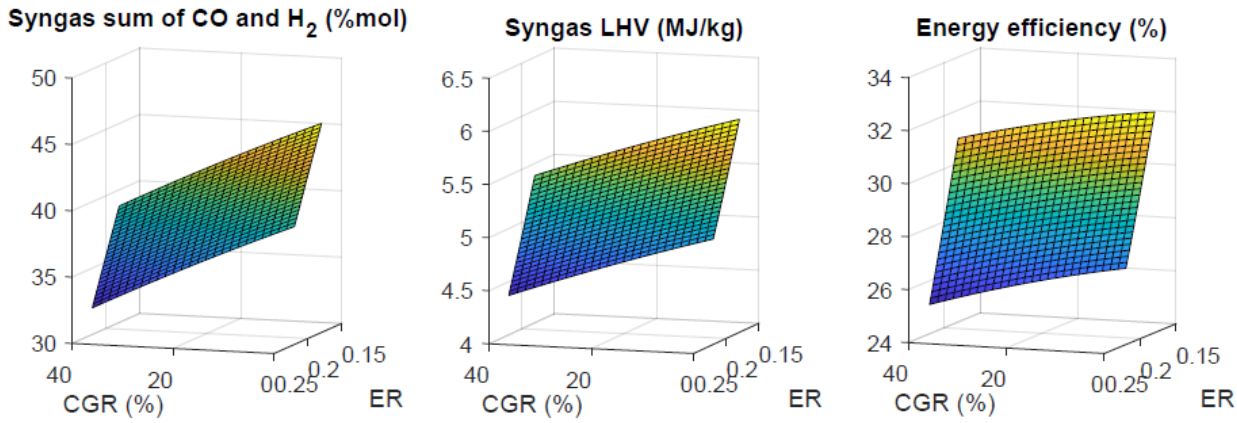


Figure 2. Response surfaces of syngas sum of CO and $H_2$ molar fractions, syngas lower heating value and energy efficiency

The resulting composition of syngas in the optimized case (0% CGR and 0.18 ER) was 5.5% $H_2O$, 25.3% CO, 10.2% $CO_2$, 20.2% $H_2$ and 1.1% $CH_4$ on a molar basis, which results in a lower heating value on a dry basis of 5.98 MJ/kg (or 6.33 MJ/Nm$^3$) and an energy efficiency of 32.2%. It shows little deviation from literature data, in which a composition in the range of 20-30% CO, 5-15% $H_2$, 5-15% $CO_2$ and 1-3% $CH_4$ is reported (Lasa et al., 2011). The syngas lower heating

value shows, as well, good agreement with reference in respect to downdraft gasification, since it was expected in the range of 4 to 7 MJ/Nm$^3$ (Sikarwar et al., 2017).

### 3.4 Comparison to the co-gasification of municipal solid waste and sugarcane bagasse

Lastly, a comparison between açaí seed and sugarcane bagasse in co-gasification with MSW was conducted in order to evaluate the potential of these two biomasses. Figure 3 presents the response surfaces for the case with sugarcane bagasse. The data referring to the co-gasification of sugarcane bagasse and MSW can be assessed in Lewin et al. (2020), with the exception that in the present study the moisture content of sugarcane bagasse and MSW were fixed at 10.4% (Vassilev et al., 2010) and 37.0%, respectively.

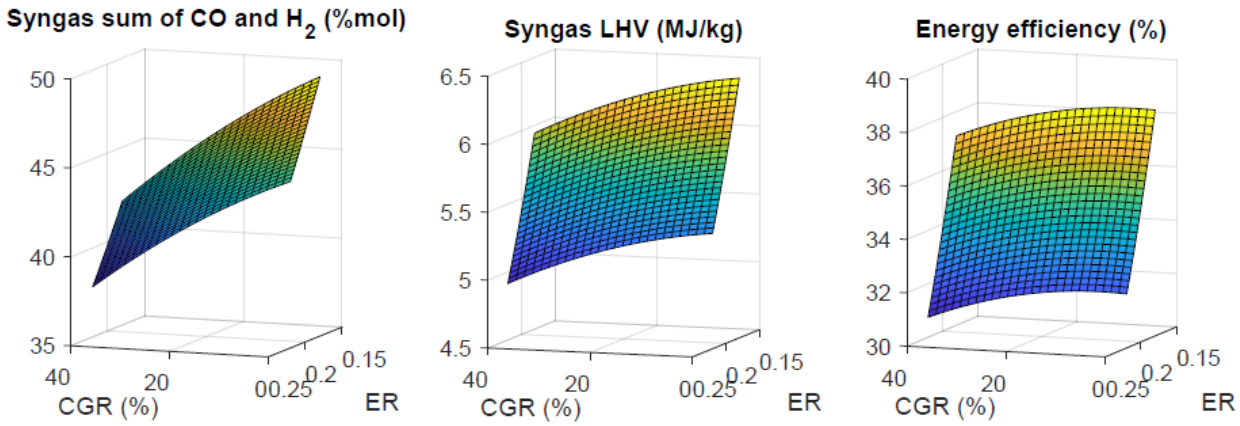


Figure 3. Response surfaces of co-gasification of MSW and sugarcane bagasse

As can be seen comparing Figure 2 and Figure **3**, all responses are higher in the case of co-gasification of MSW and sugarcane bagasse. The same optimized conditions for the case with açaí seed, 0% CGR and 0.18 ER, resulted in a composition of 4.7% $H_2O$, 27.1% CO, 9.3% $CO_2$, 19.6% $H_2$ and 1.0% $CH_4$ on a molar basis, corresponding to a LHV of 6.05 MJ/kg and an energy efficiency of 36.6%.

### 3.5 Case study: evaluating the use of municipal solid waste

In order to assess the potential of MSW outside the experimental range, two additional cases were simulated: 40% CGR and 0.15 ER, for both açaí seed and sugarcane bagasse in co-gasification with MSW. The resulting syngas compositions on a molar basis are presented in Table 8, along with the other three main responses. The high moisture content of MSW results in an $H_2$ molar fraction larger than that of the CO, but the sum of them (43.3% for açaí seed and 44.6% for sugarcane bagasse) is still high when compared to the optimized cases of 0% CGR and 0.18 ER (45.5% for açaí seed and 46.7% for sugarcane bagasse). The corresponding LHV and energy efficiency, 6.18 MJ/kg and 35.5% for açaí seed and 6.29 MJ/kg and 38.9% for sugarcane bagasse, were higher than in the optimized cases (5.98 MJ/kg and 32.2% for açaí seed and 6.05 MJ/kg and 36.6% for sugarcane bagasse), mainly because of the slightly higher $CH_4$ molar fraction, but also because of the dry basis analysis.

Table 8. Summary of the three cases compared in the present study

| | $H_2O$ (%mol) | CO (%mol) | $CO_2$ (%mol) | $H_2$ (%mol) | $CH_4$ (%mol) | $N_2$ (%mol) | CO+$H_2$ (%mol) | LHV (MJ/kg) | Energy efficiency |
|---|---|---|---|---|---|---|---|---|---|
| **60% açaí seed 40% MSW (0.15 ER)** | 9.0 | 20.7 | 13.0 | 22.6 | 1.6 | 33.1 | 43.3 | 6.18 | 35.5 |
| **60% sugarcane bagasse 40% MSW (0.15 ER)** | 8.1 | 22.1 | 12.5 | 22.5 | 1.6 | 33.3 | 44.6 | 6.29 | 38.9 |

Therefore, the co-gasification of MSW with both açaí seed and sugarcane bagasse using a CGR of 40% and an ER of 0.15 resulted in significantly good syngas, quite competitive in relation to the chosen responses. Even though the main responses were higher in the case of co-gasification with sugarcane bagasse, it has an important drawback when compared

to açaí seed, which is its lower bulk density (100 kg/m³ according to Valix et al., 2017). The bulk density of açaí seed is almost five times higher (see Table 1), enabling a less complex process of storage and transportation.

## 4. CONCLUDING REMARKS

This study evaluated the potential of co-gasification of açaí seed and municipal solid waste by modelling and simulating a downdraft gasifier operating with air in MATLAB. A central composite design of experiments $3^2$ along with some statistical analyses were employed to investigate the effects of the co-gasification ratio and equivalence ratio on the process. Polynomial models were developed for the three chosen responses, which are the sum of CO and $H_2$ molar fractions on a wet basis, the syngas lower heating value on a dry basis and the energy efficiency on a dry basis. The coefficients that presented significant effect were the independent coefficient and the linear coefficient of both CGR and ER, which presented inhibiting effect on the responses. The polynomial models showed good agreement with the results observed in MATLAB, with both $R^2$ and adjusted $R^2$ above 0.99. Response surfaces were built for all three responses, and the optimized condition that maximized the results was 0% CGR and 0.18 ER, corresponding to a syngas molar fraction of 5.5% $H_2O$, 25.3% CO, 10.2% $CO_2$, 20.2% $H_2$ and 1.1% $CH_4$.

The comparison of co-gasification of MSW and açaí seed with co-gasification of MSW and sugarcane bagasse was also addressed, and the optimized condition was also obtained for 0% MSW. The gasification of sugarcane bagasse, therefore, resulted in a composition of 4.7% $H_2O$, 27.1% CO, 9.3% $CO_2$, 19.6% $H_2$ and 1.0% $CH_4$ on a molar basis. All results were higher for sugarcane bagasse, corresponding to a LHV and energy efficiency of 6.05 MJ/kg and 36.6%, respectively, whereas for açaí seed the LHV and energy efficiency were 5.98 MJ/kg and 32.2%.

Finally, case studies of 40% CGR and 0.15 ER were conducted to evaluate the co-gasification of MSW with both açaí seed and bagasse outside the experimental range. Even though the higher moisture content of the biomass resulted in a syngas with higher $H_2O$ molar fraction, it was concluded that these conditions were competitive in relation to the chosen responses, highlighting the potential of MSW to produce energy.

## 5. ACKNOWLEDGMENTS

This study was financed in part by the Coordenação de Aperfeiçoamento de Pessoal de Nível Superior - Brasil (CAPES) - Finance Code 001. The authors would also like to thank the CNPq, FAPERJ and FINEP for the financial support to the Department of Chemical Engineering and Material (DEQM) and Department of Mechanical Engineering (DEM) at the Pontifical Catholic University of Rio de Janeiro (PUC-Rio).

## 6. REFERENCES

Associação Brasileira de Limpeza Pública e Resíduos Especiais (ABRELPE). Panorama dos Resíduos Sólidos no Brasil. 2017. Dec. 2019 < http://abrelpe.org.br/>.

Angelo, A. C. M.; Saraiva, A. B.; Climaco, J. C. M.; Infante, C. E.; Valle, R., 2017. Life cycle assessment and multi-criteria decision analysis: Selection of a strategy for domestic food waste management in Rio de Janeiro. *Journal of Cleaner Production*, Vol. 143, pp. 744-756.

Bejan, A, 2013. *Convection Heat Transfer*. John Wiley & Sons, New Jersey, 4th edition.

Bryden, K. M.; Ragland, K. W.; Rutland, C. J, 2002. "Modeling thermally thick pyrolysis of wood". *Biomass & Bioenergy*, Vol. 22, pp. 41-53.

Chaurasia, A., 2016. "Modeling, simulation and optimization of downdraft gasifier: Studies on chemical kinetics and operating conditions on the performance of the biomass gasification process". *Energy*, Vol. 116, pp. 1065-1076.

CONAB, 2019. Análise Mensal – Açaí (fruto), March 2019. May 2020 <https://www.conab.gov.br/info-agro/analises-do-mercado-agropecuario-e-extrativista/analises-do-mercado/historico-mensal-de-acai>.

De Lasa, H.; Salaices, E.; Mazumder, J.; Lucky, R., 2011. "Catalytic Steam Gasification of Biomass: Catalysts, Thermodynamics and Kinetics". *Chemical Reviews*, Vol. 111, No. 9, pp. 5404-5433.

Di Blasi, C., 2004. "Modeling Wood Gasification in a Countercurrent Fixed-Bed Reactor". *Environmental and Energy Engineering*, Vol. 50, No. 9.

Di Blasi, C., 2000. "Dynamic behaviour of stratified downdraft gasifiers". *Chemical Engineering Science*, Vol. 55, pp. 2931-2944.

Empresa de Pesquisa Energética (2019) Plano Decenal de Expansão de Energia 2029. Empresa de Pesquisa Energética, Rio de Janeiro. Dec. 2019 <http://www.epe.gov.br/sites-pt/publicacoes-dados-abertos/publicacoes/Documents/PDE%202029.pdf>.

Giltrap, D. L., 2002. *Investigating Downdraft Gasification of Biomass*. D. Sc. Thesis, Massey University, Palmerston North.

Giltrap, D. L.; Mckibbin, R.; Barnes, G. R. G., 2003. "A steady state model of gas-char reactions in a downdraft biomass gasifier". *Solar Energy*, Vol. 74, pp. 85-91.

Hoornweg, D; Bhada-Tata, P, 2012. *What a waste: A Global Review of Solid Waste Management*. Washington: Urban Development Series. Dec. 2019 <http://documents.worldbank.org/curated/pt/302341468126264791/pdf/68135-REVISED-What-a-Waste-2012-Final-updated.pdf>.

IBGE, 2018. Produção Agrícola Municipal – PAM, 2018. May 2020 <https://sidra.ibge.gov.br/pesquisa/pam/tabelas >.

Ismail, T. M.; El-Salam, M. A., 2017. "Parametric studies on biomass gasification process on updraft gasifier high temperature air gasification". *Applied Thermal Engineering*, Vol. 112, pp. 1460-1473.

Leme, M. M. V.; Rocha, M. H.; Lora, E. E. S.; Venturini, O. J.; Lopes, B. M.; Ferreira, C. H, 2014. Techno-economic analysis and environmental impact assessment of energy recovery from municipal solid waste (MSW) in Brazil. *Resources, Conservation and Recycling*, v. 87, p. 8-20.

Lewin, C. S., 2020. *Modelagem, simulação e otimização de um gaseificador de resíduos sólidos em operação cocorrente*. M. Sc. Thesis, Programa de Pós-Grasuação em Engenharia Mecânica – Centro Técnico Científico, Pontifícia Universidade Católica do Rio de Janeiro, Rio de Janeiro.

Lewin, C. S.; Martins, A. R. F. A.; Pradelle, F., 2020. Modelling, simulation and optimization of a solid residues downdraft gasifier: Application to the co-gasification of municipal solid waste and sugarcane bagasse. *Energy*, Vol. 210, 118498.

Mandl, C.; Obernberger, I.; Biedermann, F., 2010. "Modelling of an updraft fixed-bed gasifier operated with softwood pellets". *Fuel*, Vol. 89, No. 12, pp. 3795-3806.

Monteiro, A. F.; Silva, J. P. R. B.; Couto, M. A. P. G.; Teixeira, R. S. S.; Silva, A. S., 2017. "Açaí (*Euterpe oleracea*) seed biomass processing by diluted acid and enzymatic hydrolysis for sugar production". *XXI Simpósio Nacional de Bioprocessos/XII Simpósio de Hidrólise Enzimática de Biomassa* – XXI SINAFERM/ XII SHEB. Aracaju, Brazil.

Ptasinski, K. J., 2016. Efficiency of biomass energy. Hoboken: John Wiley & Sons, Inc.

Rodrigues, R., 2008. *Modelagem e simulação de um gaseificador em leito fixo para o tratamento térmico de resíduos sólidos da indústria calçadista*. M. Sc. Thesis, Programa de Pós-Graduação em Engenharia Química – Escola de Engenharia, Universidade Federal do Rio Grande do Sul, Porto Alegre.

Rodrigues, R.; Secchi, R. A.; Marcílio, N. R.; Godinho, M., 2009. "Modeling of biomass gasification applied to a combined gasifier-combustor unit: Equilibrium and kinetic approaches". *10th International Symposium on Process Systems Engineering* – PSE2009.

Santos, R. E. J., 2011. *Estudo experimental de um reator de gaseificação em um leito fixo de açaí*. M. Sc. Thesis, Programa de Pós-Graduação em Engenharia Mecânica – Instituto de Tecnologia, Universidade Federal do Pará, Belém.

Sikarwar, V. S.; Zhao, M.; Fennell, P. S.; Shah, N.; Anthony, E. J, 2017. "Progress in biofuel production from gasification". *Progress in Energy and Combustion Science*, Vol. 61, pp. 189-248.

Situmorang, Y. A.; Zhao, Z.; Yoshida, A.; Abudula, A., 2020. "Small-scale biomass gasification systems for power generation (<200 kW class): A review". *Renewable and Sustainable Energy Reviews*, Vol. 117, 109486.

Speight, J. G, 2010. *The Biofuels Handbook*. Great Britain: Royal Society of Chemistry.

Valix, M.; Katyal, S.; Cheung, W. H, 2017. Combustion of thermochemically torrefied sugar cane bagasse. *Bioresource Technology*, Vol. 223, pp. 202-209.

Vassilev, S V.; Baxter, D.; Andersen, L. K.; Vassileva, C. G., 2010 An overview of the chemical composition of biomass. *Fuel*, Vol. 89, n. 5, pp. 913-933.

Yucel, O.; Hastaoglu, M. A., 2016. "Kinetic modeling and simulation of throated downdraft gasifier". *Fuel Processing Technology*, Vol. 144, pp. 145-154.

## 7. RESPONSIBILITY NOTICE

The authors are the only responsible for the printed material included in this paper.